16th Australasian Fluid Mechanics Conference
Crown Plaza, Gold Coast, Australia
2-7 December 2007

On the Natural Convection Boundary Layer Adjacent to an Inclined Flat Plate Subject to Ramp Heating

S.C. Saha, C. Lei and J.C. Patterson

School of Engineering
James Cook University, Townsville, QLD 4811, AUSTRALIA

Abstract

An investigation of the natural convection boundary layer adjacent to an inclined semi-infinite plate subject to a temperature boundary condition which follows a ramp function up until some specified time and then remains constant is reported. The development of the flow from start-up to a steady-state has been described based on scaling analyses and verified by numerical simulations. Attention in this study has been given to fluids having a Prandtl number *Pr* less than unity. The boundary layer flow depends on the comparison of the time at which the ramp heating is completed and the time at which the boundary layer completes its growth. If the ramp time is long compared with the steady state time, the layer reaches a quasi steady mode in which the growth of the layer is governed solely by the thermal balance between convection and conduction. On the other hand, if the ramp is completed before the layer becomes steady; the subsequent growth is governed by the balance between buoyancy and inertia, as for the case of instantaneous heating.

Introduction It is well known that natural convection heat transfer occurs as a result of temperature differences in an enclosure or near a heated or cooled flat plate. Natural convection along an inclined plate has received less attention than the cases of vertical and horizontal plates. However, this configuration is very frequently encountered in engineering devices and in the natural environment. A number of researchers have considered an inclined, semi infinite flat plate in their research because of its engineering applications. Some of these are [1, 2, 7, 9]. Most of these studies have been conducted by either numerical simulations or experimental observations. There is no evidence of investigation of such problems using scaling analyses to obtain the transient flow behavior which is of great fundamental interest and of practical importance.

Scaling has been used by many researchers to discover the transient flow development for different kinds of geometries and thermal forcing. To accomplish this in a compact and effective format is the objective of this article. Scale analysis is a cost-effective approach that can be applied as a first step in understanding the physics behind the fluid flow and heat transfer issues. The results of scale analysis can serve as a guide for both experimental and numerical investigations.

An extensive investigation of the transient behavior of natural convection of a two dimensional side-heated rectangular cavity has been carried out by Patterson & Imberger [4]. Schladow, Patterson & Street [8] conducted a series of two- and three-dimensional numerical simulations of transient flow in a side-heated cavity and their simulations generally agree with the results of the scaling arguments developed by Patterson & Imberger [4].

Lei & Patterson [3] present a scaling analysis and establish relevant scales to quantify the flow properties in different flow regimes of the unsteady natural convection flow in a gently sloped shallow wedge induced by the absorption of solar radiation. The authors classify the flow development largely into one of three regimes: a conductive regime, a transitional regime and a convective regime, depending on the Rayleigh number. Poulikakos & Bejan [5] reported the outcome of a study on thermal convection inside a half isosceles triangular cavity with a cold upper wall, a hot horizontal bottom, and an insulated vertical wall. The transient behavior of the fluid is examined based on scaling analyses. The transient phenomenon begins with a sudden cooling of the upper slopped wall. It was shown that both walls develop hydrodynamic and thermal boundary layers whose thicknesses increase towards steady-state values.

From the above review, it is found that the behavior of the transient flow due to ramp heating, which increases linearly over a certain time period and is then followed by constant heating, has not yet been investigated. In this study, an investigation of the natural convection boundary layer adjacent to an inclined flat plate subject to ramp heating is carried out to develop scaling relations for characterizing the flow behavior at different stages of the flow development. These scaling relations are then validated by a series of numerical simulations with selected values of the Prandtl number (*Pr*) and Grashof number (*Gr*) in the ranges of $0.05 \leq Pr \leq 0.5$ and $1.44\times10^5 \leq Gr \leq 4.24\times10^7$ and with a fixed aspect ratio $A = 0.5$.

Problem Formulation

The physical system sketched in figure 1 consists of an inclined flat plate (*AB*). We extend both sides of the plate equal to its length and form a rectangular domain which is filled with a fluid at a temperature T_c. If we consider the plate as the hypotenuse of a right angled triangle then the altitude is h, the length of the base is l and the angle of the plate that makes with the base is θ.

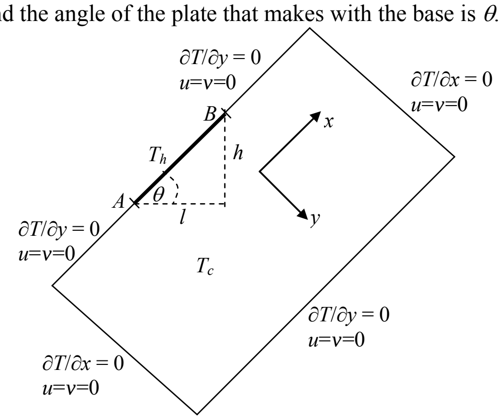

Figure 1. Schematic of the boundary layers developing along the inclined wall.

Except for the plate (the *AB* section shown in figure 1) all other walls of the rectangle are assumed to be adiabatic. At the time t = 0, the plate temperature and the inside temperatures are the same. The temperature on the plate then increases according to a ramp function for a certain period of time, after which a constant temperature is maintained.

Under the Boussinesq approximations the governing continuity, momentum and the energy equations take the following forms.

$$\frac{\partial u}{\partial x}+\frac{\partial v}{\partial y}=0 \tag{1}$$

$$\frac{\partial u}{\partial t}+u\frac{\partial u}{\partial x}+v\frac{\partial u}{\partial y}=-\frac{1}{\rho}\frac{\partial p}{\partial x}+\nu\left(\frac{\partial^2 u}{\partial x^2}+\frac{\partial^2 u}{\partial y^2}\right)+g\beta\sin\theta(T-T_h) \tag{2}$$

$$\frac{\partial v}{\partial t}+u\frac{\partial v}{\partial x}+v\frac{\partial v}{\partial y}=-\frac{1}{\rho}\frac{\partial p}{\partial y}+\nu\left(\frac{\partial^2 v}{\partial x^2}+\frac{\partial^2 v}{\partial y^2}\right)-g\beta\cos\theta(T-T_h) \tag{3}$$

$$\frac{\partial T}{\partial t}+u\frac{\partial T}{\partial x}+v\frac{\partial T}{\partial y}=\kappa\left(\frac{\partial^2 T}{\partial x^2}+\frac{\partial^2 T}{\partial y^2}\right) \tag{4}$$

where u and v are the velocity components parallel and normal to the inclined surface respectively. T is the temperature and p is the pressure, t is the time, g is the acceleration due to gravity, θ is the angle of the inclined plate with the horizontal base, and ν, ρ, β and κ the kinematic viscosity, density, coefficient of thermal expansion and thermal conductivity of the fluid respectively.

The thermal boundary condition on the heated plate is define as

$$T_h=\begin{cases}T_c & \text{if } t\le 0;\\ T_c+\Delta T(t/t_p) & \text{if } 0<t\le t_p;\\ T_c+\Delta T & \text{if } t>t_p;\end{cases}$$

where t_p is the length of the ramp heating function.

Scaling Analysis

Thermal Layer Development

The start-up stage is initially dominated by heat transfer via conduction through the hot plate, resulting in a thermal boundary layer of a thickness $O(\delta_T)$. Within the boundary layer the dominant balance is that between the thermal inertia term and the y diffusion term in the energy equation (4):

$$\frac{\Delta T}{t}\sim\kappa\frac{\Delta T}{\delta^2}$$

$$\Rightarrow\ \delta_T\sim\kappa^{1/2}t^{1/2} \tag{5}$$

In Eqn (2) the unsteady inertia term is of $O(u/t)$, viscous term $O(\nu u/\delta_T^2)$, advection term $O(u^2/AB)$. The ratio of the advection term to the unsteady term is $O(ut/AB)$. For very small time $ut/AB<<1$. Therefore the advection term is not significant for small time. The ratio of the unsteady to the viscous terms is $(u/t)/(\nu u/\delta_T^2)\sim\delta^2/(\nu t)\sim 1/Pr$. Where $Pr=\nu/\kappa$. For $Pr<<1$ the viscous term is much smaller than the unsteady term and the correct balance is between the unsteady and buoyancy terms. However $Pr>>1$ the unsteady term is much smaller than the viscous term and the correct balance is between viscosity and buoyancy. If $Pr\sim O(1)$, then the unsteady and viscous terms are of the same order and both terms need to be included in a balance with the buoyancy term.

$$(1+Pr)\frac{u}{t}\sim g\beta\sin\theta\Delta T_m\frac{t}{t_p}$$

$$\Rightarrow\ u\sim\frac{g\beta\sin\theta\Delta Tt^2}{(1+Pr)t_p}$$

$$\sim\frac{g\beta\cos\theta\tan\theta\Delta Tt^2}{(1+Pr)t_p}$$

The slope or aspect ratio is $\tan\theta=A$ and $\cos\theta=l/(l^2+h^2)^{1/2}=1/(1+A^2)^{1/2}$. Hence,

$$u\sim\frac{ARaPr}{(1+Pr)(1+A^2)^{1/2}}\left(\frac{t}{h^2/\kappa}\right)\left(\frac{t}{t_p}\right)\left(\frac{\kappa}{h}\right) \tag{6}$$

Now the balance in the inclined momentum equation holds as long as $t<t_p$, where the Rayleigh number is defined by $Ra=g\beta\Delta Th^3/(\kappa\nu)$. This continues until the balance between convection and conduction occurs at time t_s

$$\frac{u}{l/\cos\theta}\Delta T\frac{t_s}{t_p}\sim\kappa\frac{\Delta T}{\delta^2}\frac{t}{t_p}$$

$$\Rightarrow u\sim\frac{\kappa l}{\kappa t_s\cos\theta}$$

$$\sim\frac{h}{At_s\cos\theta} \tag{7}$$

Using the boundary layer thickness scale (5) and the velocity scales (6) and (7) we conclude that the growth of the thermal boundary layer along the top wall ends at time t_s when

$$\frac{ARaPr}{(1+Pr)(1+A^2)^{1/2}}\left(\frac{t_s}{h^2/\kappa}\right)\left(\frac{t_s}{t_p}\right)\left(\frac{\kappa}{h}\right)\sim\frac{h}{At_s\cos\theta}$$

$$\Rightarrow\ t_s^3\sim\frac{h^4t_p(1+Pr)(1+A^2)}{A^2RaPr\kappa^2\cos\theta}$$

$$\Rightarrow\ t_s\sim\frac{(1+Pr)^{1/3}(1+A^2)^{1/3}}{A^{2/3}Ra^{1/3}Pr^{1/3}}\left(\frac{t_p}{h^2/\kappa}\right)^{1/3}\left(\frac{h^2}{\kappa}\right) \tag{8}$$

so long as $t_s<t_p$. This is the same as saying that $t_p>(1+Pr)^{1/2}(1+A^2)^{1/2}h^2/[A(RaPr)^{1/2}\kappa]$, which is the steady state time for an instantaneous function start up (see [6]). This means that if the ramp time is longer than the time it would have taken for the step function start up to reach a steady state boundary layer, then the boundary layer will have reached a balance before the ramp has finished.

The thickness of the boundary layer along the plate at the steady state time is

$$\delta_T\sim\kappa^{1/2}\frac{(1+Pr)^{1/6}(1+A^2)^{1/6}}{A^{1/3}(RaPr)^{1/6}}\left(\frac{t_p}{h^2/\kappa}\right)^{1/6}\left(\frac{h^2}{\kappa}\right)^{1/2}$$

$$\sim\frac{\kappa^{1/6}h^{2/3}t_p^{1/6}(1+Pr)^{1/6}(1+A^2)^{1/6}}{A^{1/3}(RaPr)^{1/6}}$$

$$\sim\frac{h(1+Pr)^{1/6}(1+A^2)^{1/6}}{A^{1/3}(RaPr)^{1/6}}\left(\frac{t_p}{h^2/\kappa}\right)^{1/6} \tag{9}$$

At the time when the plate boundary layer is steady, the u velocity scale is

$$u\sim\frac{(RaPr)^{1/3}(1+A^2)^{1/6}}{A^{1/3}(1+Pr)^{1/3}}\left(\frac{h^2/\kappa}{t_p}\right)^{1/3}\left(\frac{\kappa}{h}\right) \tag{10}$$

On the other hand, if $t_p<(1+Pr)^{1/2}(1+A^2)^{1/2}h^2/[A(RaPr)^{1/2}\kappa]$, then $t_s>t_p$ and the thermal boundary layer has not finished growing when the ramp finishes. This means that the boundary layer grows as though the startup were instantaneous and reaches a steady state at $(1+Pr)^{1/2}(1+A^2)^{1/2}h^2/[A(RaPr)^{1/2}\kappa]$, and there is no difference between the ramp and instantaneous start up cases.

In the former case with the start up time less than the ramp time, once t_s is reached, then the boundary layer stops growing according to $\kappa^{1/2}t^{1/2}$. The thermal boundary layer is in a quasi steady mode with convection balancing conduction, and (viscosity + unsteady) balancing buoyancy. Further increase of the heat input simply accelerates the flow to maintain the proper thermal balance. For the ramp function startup, this means that

$$\frac{u}{l/\cos\theta}\Delta T\frac{t_s}{t_p} \sim \kappa\frac{\Delta T}{\delta^2}\frac{t_s}{t_p}$$

$$\Rightarrow\ u \sim \frac{\kappa d}{\delta^2 \cos\theta} \qquad (11)$$

At this time the unsteady term is not important. Therefore,

$$\nu\frac{u}{\delta^2} \sim g\beta\sin\theta\Delta T\frac{t}{t_p}$$

$$\Rightarrow\ \nu\frac{\kappa L}{\delta^4\cos\theta} \sim g\beta\sin\theta\Delta T\frac{t}{t_p}$$

$$\Rightarrow\ \delta^4 \sim \frac{h^4 t_p}{ARa\cos\theta\sin\theta\, t}$$

$$\Rightarrow\ \delta \sim \frac{h\left(1+A^2\right)^{1/4}}{A^{1/2}Ra^{1/4}}\left(\frac{t_p}{t}\right)^{1/4} \qquad (12)$$

where $\sin\theta = h/(l^2+h^2)^{1/2} = A/(1+A^2)^{1/2}$, and

$$u \sim Ra^{1/2}\left(\frac{\kappa}{h}\right)\left(\frac{t}{t_p}\right) \qquad (13)$$

At $t \sim t_p$, (12) and (13) become the same scales as those for the step function start up, so the only difference between the ramp and step function start up is what happens between t_s and t_p. After t_p, the boundary layer does not know that it started up from a ramp. Notice that the boundary layer thickness decreases beyond t_p. This has to happen as the fluid is accelerating and is therefore more effective in convecting the heat away; the boundary layer has to contract so that conduction is increased to balance that.

Viscous Layer Development

Balance between viscous and inertia terms of the momentum equation

$$\delta_v \sim \nu^{1/2}t^{1/2} \sim Pr^{1/2}\delta_T \qquad (14)$$

When $Pr < 1$ then δ_v will be always smaller than δ_T, that means the viscous boundary layer is always embedded within the thermal boundary layer. The opposite case happens when $Pr > 1$. When the thermal layer has reached the steady state, the viscous layer has a thickness of order

$$\delta_v \sim Pr^{1/3}\frac{h\left(1+\mathrm{Pr}\right)^{1/6}\left(1+A^2\right)^{1/6}}{A^{1/3}Ra^{1/6}}\left(\frac{t_p}{h^2/\kappa}\right)^{1/6} \qquad (15)$$

Numerical Procedure

In order to validate the scales derived in the previous section, a series of numerical simulations have been carried out for the cases described in Table 1. Equations (1) - (4) are solved along with the initial and boundary conditions using the SIMPLE scheme in Fluent 6.3.26, in which the spatial derivatives are discretized with a second order upwind scheme and the diffusion terms with a second order center-differenced scheme. The temporal derivatives are discretized with a second order implicit scheme. To ensure that a sufficiently high accuracy is achieved in the numerical simulations, a non-uniform computational mesh has been used which concentrates points in the boundary layer and near the plate and is relatively coarse in the interior of the big domain.

Mesh and time step dependence tests have been carried out to ensure the accuracy of the numerical solutions. The time steps have been chosen in such a way that the CFL (Courant-Freidrich-Lewy) number remains the same for all meshes. The tests are conducted for the highest Grashof number case. It is expected that the selected mesh for the highest Grashof number is also appropriate for the lower Grashof numbers. Four different mesh sizes have been tested for A = 0.5. The time histories of the calculated velocity with four different meshes are plotted in figure 2. The maximum variation of the velocity between the coarsest and finest meshes is 0.54%. Therefore any of these meshes is appropriate for this simulation, and the mesh size of 340×200 is adopted for the whole range of simulation.

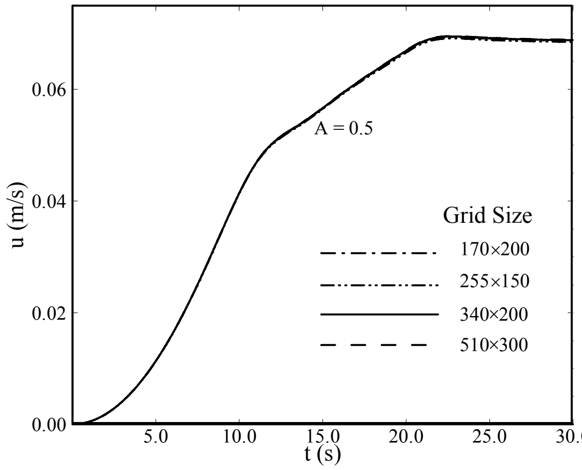

Figure 2: Time series of the maximum velocity parallel to the inclined surface calculated on the line normal to the surface at the mid point for A = 0.5 while $Gr = 4.24\times10^7$ and Pr = 0.72.

Validation of the scaling

A total of ten simulations have been performed to verify the scaling relations. Table 1 shows the details of the flow parameters considered for this study. Here, Runs 1-7 with $Gr = 4.24\times10^7$, 1.06×10^7, 8.48×10^6, 4.24×10^6, 2.15×10^6, 1.80×10^6 and 1.44×10^6 while keeping A = 0.5 and Pr = 0.72 unchanged have been carried out to show the dependence of the scaling relations on the Grashof number Gr; and Runs 8-10 and Run 1 with Pr = 0.5, 0.1, 0.05 and 0.72 while keeping A = 0.5 and $Gr = 4.24\times10^7$ unchanged have been carried out to show the dependence of the scaling relations on the Prandtl number Pr.

The velocity parallel to the plate and the temperature have been recorded at several locations along a line perpendicular to the plate at the mid point to obtain the velocity and temperature profiles. The maximum velocity parallel to the plate has been calculated as a characteristic velocity (u) along that line. This velocity is used to verify the velocity scale relation.

Table1: Values of *Gr* and *Pr* for the 10 runs

Runs	*Gr*	*Pr*
1	4.24×10^7	0.72
2	1.06×10^7	0.72
3	8.48×10^6	0.72
4	4.24×10^6	0.72
5	2.15×10^6	0.72
6	1.80×10^6	0.72
7	1.44×10^6	0.72
8	4.24×10^7	0.5
9	4.24×10^7	0.1
10	4.24×10^7	0.05

Time series of the maximum velocity parallel to the inclined surface calculated on the line normal to the surface at the mid point for A = 0.5 are shown in figure 2 with $Gr = 4.24\times10^7$ and Pr = 0.72. These velocities are calculated for four different mesh sizes. The ramp time has been set to 20s. As is mentioned in the scaling analysis, the ramp time may be larger or smaller than the steady state time for the boundary layer. If the ramp time is larger than the steady state time, then after that time the velocity continues to increase as the plate is still being heated up. in this figure that at about 11.5s the boundary layer becomes quasi steady. However, the velocity still increases as the temperature on the plate is still increasing. At t = 20s the ramp finishes and the boundary layer becomes completely steady at about 22s.

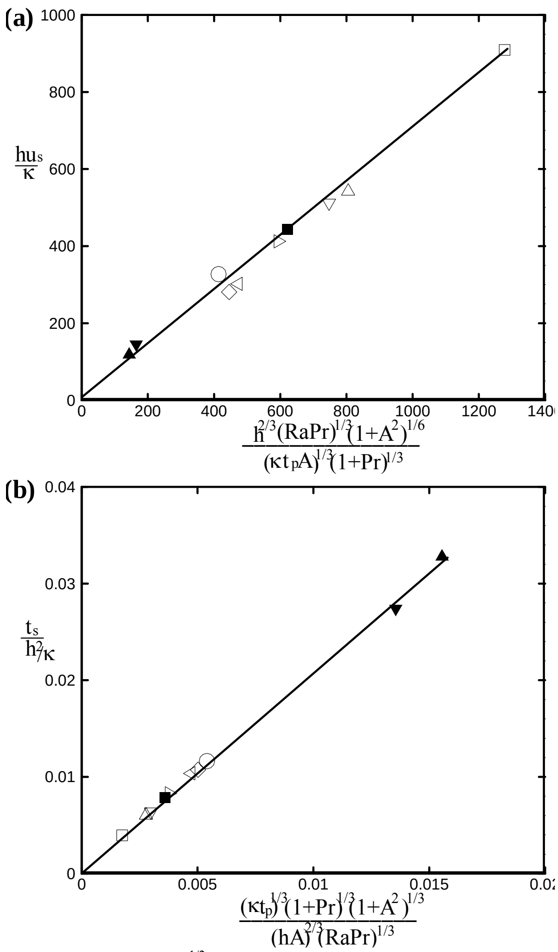

Figure 3. (a) $hu_s/(\kappa Ra^{1/2})$ plotted against $h^{2/3}(RaPr)^{1/3}(1+A^2)^{1/6}/[(\kappa t_p A)^{1/3}(1+Pr)^{1/3}]$; (b) $t_s/(h^2/\kappa)$ plotted against $(\kappa t_p)^{1/3}(1+Pr)^{1/3}(1+A^2)^{1/3}/[(hA)^{2/3}(RaPr)^{1/3}]$; □, run 1; Δ, run 2; ∇, run 3; ▷, run 4; ◁, run 5; ◊, run 6; o, run 7; ■, run 8; ▲, run 9; ▼, run 10. Solid line, linear fit.

Numerical results of the scaling laws for the steady state time and the velocity parallel to the plate, (8) and (10) respectively are presented in figure 3. It is seen in the figure 3 that the numerical results agree very well with the scaling relations. For all the cases calculated in this study, the numerical results fall approximately onto a straight line, which confirms that the scaling relations (8) and (10) properly describe the boundary layer in the steady state.

Conclusions

The natural convection boundary layer adjacent to an inclined semi-infinite plate subject to a temperature boundary condition which follows a ramp function up until a specified time, and then remains constant, has been investigated. The boundary layer flow depends on the comparison of the time at which the ramp heating is completed with the time at which the boundary layer completes its growth. If the ramp time is long compared with the steady state time, the thermal boundary layer reaches a quasi steady mode in which the growth of the layer is governed solely by the

However, the growth rate of the velocity is smaller compared to the velocity during the earlier phase. The two-stage growth of the velocity is clearly seen in the simulation (see figure 2). It is seen

thermal balance between convection and conduction. On the other hand, if the ramp is completed before the thermal boundary layer becomes steady; the subsequent growth is governed by the balance between buoyancy and inertia, as for the case of instantaneous heating. Several scaling relations have been established in this study, which include the maximum velocity parallel to the inclined plate inside the boundary layer (u), the time for the boundary layer to reach the steady state (t_s) and the thermal and viscous boundary layer thicknesses (δ_T and δ_v). The comparisons between the scaling relationships and the numerical simulations demonstrate that the scaling results agree very well with the numerical simulations. Hence the numerical results have confirmed the scaling relations properly describe the overall flow development.

Acknowledgments

This research is supported by the Australian Research Council.

References

[1] Ganesan, P. & Palani, G., Natural convection effects on impulsively started inclined plate with heat and mass transfer, *Heat and Mass Transfer*, **39**, 2003, 277–283.

[2] Ganesan, P. & Palani, G., Finite difference analysis of unsteady natural convection MHD flow past an inclined plate with variable surface heat and mass flux, *Int. J. Heat Mass Transfer*, **47**, 2004, 4449–4457.

[3] Lei, C. & Patterson, J. C., Unsteady natural convection in a triangular enclosure induced by absorption of radiation. *J. Fluid Mech.* **460**, 2002, 181–209

[4] Patterson, J. C. & Imberger, J. Unsteady natural convection in a rectangular cavity, *J. Fluid Mech*., **100**, 1980, 65.

[5] Poulikakos, D. and Bejan, A., The fluid dynamics of an attic space, *J. Fluid Mech*., **131**, 1983, 251–269.

[6] Saha, S. C., Lei, C. & Patterson, J. C., Scaling Analysis of the Thermal Boundary Layer Adjacent to an Abruptly Heated Inclined Flat Plate. Submitted to the 16*th Australasian Fluid Mechanics Conference*. University of Queensland, Australia. 2007

[7] Said, S. A. M., Habib, M. A., Badr, H. M. & Anwar, S., Turbulent natural convection between inclined isothermal plates, *Computers & Fluid*, **34**, 2005, 1025–1039.

[8] Schladow, S. G., Patterson, J. C. & Street, R. L., Transient flow in a side- heated cavity at high Rayleigh number: A numerical study. *J. Fluid Mech.*, **200**, 1989, 121-148

[9] Sparrow, E. M. and Husar, R. B., Longitudinal vortices in natural convection flow on inclined plates, *J. Fluid. Mech.*, **37**, 1969, 251–255.